

Article

Removal of Ionic Liquids from Oil Sands Processing Solution by Ion-Exchange Resin

Hong Sui^{1,2,3}, Jingjing Zhou^{1,2}, Guoqiang Ma^{1,2} , Yaqi Niu¹, Jing Cheng⁴, Lin He^{1,2,*} and Xingang Li^{1,2,3}

¹ School of Chemical Engineering and Technology, Tianjin University, Tianjin 300072, China; suihong@tju.edu.cn (H.S.); zhoujj.zm@gmail.com (J.Z.); zxmaggq@gmail.com (G.M.); niuyaqi@tju.edu.cn (Y.N.); lxg@tju.edu.cn (X.L.)

² National Engineering Research Center of Distillation Technology, Tianjin 300072, China

³ Collaborative Innovation Center of Chemical Science and Engineering, Tianjin 300072, China

⁴ China Petroleum Pipeline Engineering Co. Ltd. Tianjin Branch, Tianjin 300000, China; cchengjing@cnpc.com.cn

* Correspondence: linhe@tju.edu.cn; Tel.: +86-022-2740-4701

Received: 29 July 2018; Accepted: 6 September 2018; Published: 11 September 2018



Featured Application: The work provides some fundamental understanding on the pretreatment and concentration of the ionic liquids solution, especially those with extremely low concentration of ionic liquids. This kind of method could be potentially combined with other methods, such as distillation, crystallization, etc., in the removal or recovery or purification of ionic liquids from solutions or waste solids.

Abstract: Ionic liquids (ILs) have been reported to be good process aids for enhanced bitumen recovery from oil sands. However, after the extraction, some ionic liquids are left in the residual solids or solutions. Herein, a washing–ion exchange combined method has been designed for the removal of two imidazolium-based ILs, ([Bmim][BF₄] and [Emim][BF₄]), from residual sands after ILs-enhanced solvent extraction of oil sands. This process was conducted as two steps: water washing of the residual solids to remove ILs into aqueous solution; adsorption and desorption of ILs from the solution by the sulfonic acid cation-exchange resin (Amberlite IR 120Na). Surface characterization showed that the hydrophilic ionic liquids could be completely removed from the solid surfaces by 3 times of water washing. The ionic liquids solution was treated by the ion-exchange resin. Results showed that more than 95% of [Bmim][BF₄] and 90% of [Emim][BF₄] could be adsorbed by the resins at 20 °C with contact time of 30 min. The effects of some typical coexisted chemicals and minerals, such as salinity, kaolinite (Al₄[Si₄O₁₀](OH)₈), and silica (SiO₂), in the solution on the adsorption of ionic liquids have also been investigated. Results showed that both kaolinite and SiO₂ exerted a slight effect on the uptake of [Bmim][BF₄]. However, it was observed that increasing the ionic strength of the solution by adding salts would deteriorate the adsorption of [Bmim]⁺ on the resin. The adsorption behaviors of two ILs fit well with the Sips model, suggesting the heterogeneous adsorption of ionic liquids onto resin. The adsorption of ionic liquids onto Amberlite IR 120Na resin was found to be pseudo-second-order adsorption. The regeneration tests showed stable performance of ion-exchange resins over three adsorption–desorption cycles.

Keywords: ionic liquids; ion-exchange resin; adsorption; removal; residual sand; washing

1. Introduction

Ionic liquids (ILs) are a kind of organic salt with low melting points (mainly <100 °C). Generally, the ILs are composed of organic cations and organic/inorganic anions. In the past few years, ILs have

attracted increasing attention of researchers due to their unique characteristics, such as low vapor pressure, non-flammability under ambient conditions, high solvent capacity, a wide electrochemical window, and so forth [1,2]. The physical and chemical properties (e.g., solubility, polarity, viscosity, and acidity) of ILs could be designed simply by careful selection of the ions, thereby allowing “IL tailoring” for a particular application [3]. These unique and versatile properties suggest ILs as potential substituents for traditional volatile organic solvents in a wide range of fields such as synthesis and separation [4,5].

Recently, some imidazolium-based ILs have been used to enhance solvent extraction of bitumen from oil sands. Compared to conventional solvent extraction, bitumen recovery could be highly improved (at least 10%) with the assistance of ILs. In addition, due to the strong surface modification by the ionic liquids, the mineral surfaces become more hydrophilic, allowing much less clay and fines to be entrained into the recovered bitumen [6–9]. However, during the ILs-assisted solvent extraction, there are still some ionic liquids being attached in the residual solids due to the direct contact with the minerals. Our previous results showed that these residual ionic liquids in the waste solids could be washed away by water because of their hydrophilicity. Unfortunately, much more detailed investigation on how to remove these ionic liquids from the residual solids is still needed.

To recover the ionic liquids from solutions, different kinds of methods have been proposed, such as distillation [10,11], extraction [12,13], aqueous two-phase systems [14,15], membrane technology [16,17], adsorption [18,19], and so on. The adsorption is regarded as an eco-friendly and cost-effective way. Among the reported adsorbents (e.g., activated carbons [20,21], clays [22], and bacterial biosorbents [23], etc.), ion-exchange resins are considered to be candidates for treatment of low-concentration ionic liquids solutions [24–27] due to the high adsorption efficiency and reusability. Sun et al. [24] investigated removal of the cationic part of 1-ethyl-3-methylimidazolium acetate ([Emim][OAc]) from aqueous solution by twelve ion-exchange resins. The sulfonic acid ion-exchange resins showed the most efficient adsorption, while the particle size and crosslinking degree of resin exerted slight influence on the uptake of [Emim] cations. Li and coworkers [25] demonstrated that the anions of imidazolium-based ILs insignificantly affected the adsorption performance of ion-exchange resins, and enhanced adsorption capacity was observed for ILs with longer alkyl chains. However, the regeneration and reusing of the ion-exchange resins were not studied in their work. He et al. [27] used ion-exchange resin to recover three benzothiazolium ILs from coexisting glucose, but the adsorption mechanisms of ILs onto ion-exchange resins were still unclear.

Accordingly, the aims of this study are to: (i) investigate the effect of operation parameters and water chemistry on ILs adsorption onto ion-exchange resin after oil–solid separation; (ii) understand the adsorption mechanisms of ILs onto ion-exchange resin; (iii) test the regeneration and recyclability of ion-exchange resin.

2. Experimental Section

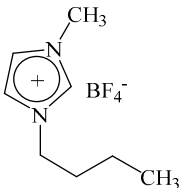
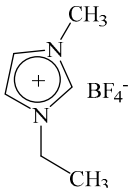
2.1. Materials

The ion-exchange resin (Amberlite IR 120Na) was provided by the Dow Chemical Company (Philadelphia, PA, USA). The physical and chemical properties of the resin are presented in Table 1. Two ILs ([Bmim][BF₄], [Emim][BF₄]) were purchased from Lanzhou Institute of Chemical Physics, Chinese Academy of Sciences (Lanzhou, China) with purity of 99%, which are listed in Table 2. Other reagents, including sodium chloride, calcium chloride, hydrochloric acid, kaolinite, silica (40–60 mesh), at their analytical grade, were purchased from Yuanli Technology Co. Ltd. (Tianjin, China). The deionized (DI) water used in this work had a resistivity of 18 MΩ·cm.

Table 1. Physical and chemical properties of ion-exchange resin (Amberlite IR 120Na).

Matrix	Type	Functional Group	Total Exchange Capacity	Ionic Form as Shipped	Particle Size	Moisture Content	Shipping Weight	Physical Form
Styrene divinylbenzene copolymer	Gel	Sulfonic acid	≥2.0 eq/L (Na ⁺ form)	Na ⁺	0.6~0.8 mm	45~50%	840 g/L	Amber spherical beads

Table 2. Physical and chemical properties of ionic liquids used in this study.

Ionic Liquids	1-Butyl-3-Methylimidazolium Tetrafluororate	1-Ethyl-3-Methylimidazolium Tetrafluororate
Molecular structure		
Acronym	[Bmim][BF ₄]	[Emim][BF ₄]
Chemical formula	C ₈ H ₁₅ BF ₄ N ₂	C ₆ H ₁₁ BF ₄ N ₂
Molecular weight (g/mol)	226.02	197.97
Viscosity (cP)	153.8 (298.1 K)	66.5 (298.1 K)
Density (g/mL)	1.171 (298.1 K) [28]	1.248 (298.1 K) [6]

2.2. Ionic Liquid Solution Samples

The ionic liquid samples were prepared in two different ways: the real washing samples and the model samples. The real washing samples were obtained by washing the residual solids after the hybrid extraction of oil sands. The detailed hybrid extraction of oil sands by ionic liquids (i.e., [Bmim][BF₄] and [Emim][BF₄]) and solvent is given in our previous study [6]. The residual sands were firstly transferred to a sand core funnel (G4). Then the water was added to a funnel for four times, with a certain volume of 20 mL for each time. The residual sands were filtered under vacuum after each time of addition of water. The ILs were removed to the solution from the residual sands. When the filtration was finished, the residual sands were dried in an oven for 4 h at 105 °C and reserved for further analysis.

To quantitatively investigate the adsorption behaviors of ionic liquids onto the resins, model ionic liquids solution samples were prepared based on the real washing samples. ILs were transferred to a volumetric flask and diluted to 1000 mL with DI water.

2.3. Adsorption of ILs onto Ion-Exchange Resins

The ion-exchange resin (Amberlite IR 120Na) was used to remove ILs from the solution by batch adsorption. During the adsorption process, the adsorbate ions transfer from the bulk liquid phase to a porous adsorbent in three consecutive steps: (i) mass transfer of the adsorbate ions through the boundary layer film of liquid to the external surface of adsorbent (film diffusion); (ii) diffusion of the adsorbate ions within the liquid-filled pores of adsorbent (intraparticle diffusion); (iii) adsorption of the adsorbate ions through ion exchange on the internal or external surface of the adsorbent [29]. The ion exchange process is illustrated in Figure 1. The matrix of the ion-exchange resin is the styrene divinylbenzene copolymer, where styrene is the monomer and divinylbenzene is the crosslinking agent. The functional group of the resin is sulfonic acid. When ion-exchange resin is introduced to ILs solution, H⁺ of the sulfonic acid has been exchanged with the cationic part (represented by A⁺) of ILs, thus allowing the adsorption of IL cations onto the ion-exchange resin. Simultaneously, the H⁺ ions

are released from the resin and transferred into the bulk aqueous solution. The adsorption process can be expressed by Equation (1):

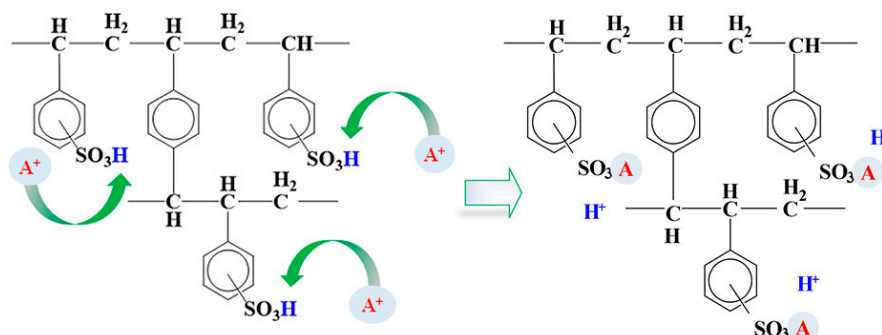


Figure 1. Ion exchange process of cationic part of ionic liquids (represented by A⁺) with the H⁺ on ion-exchange resin (Amberlite IR 120Na).

Before the adsorption, the ion-exchange resin was pretreated by being immersed in NaCl aqueous solution (15 wt%) for 12 h. This treatment avoids the breaking of resin caused by water uptake. After the salt pretreatment, the resin was further soaked in diluted HCl aqueous solution (5 wt%) for 4 h to transform the ionic form from Na⁺ to H⁺. Subsequently, the resin was washed by DI water until the pH of the water was about 7.

The pretreated ion-exchange resins were added into glass conical flasks (250 mL) containing ILs solution (150 mL). The mixture was stirred at 250 rpm under ambient conditions (20 °C) for 30 min in a temperature-controlled water bath to allow the adsorption to reach the equilibrium state. Subsequently, the resins were separated from the solution by filtration. The concentration of the residual ILs in filtrate was determined using ultraviolet-visible (UV-vis) spectrophotometry. The influences of operation parameters such as resin dose, temperature, and contact time were investigated to optimize the adsorption process. The isotherms and kinetics of ILs adsorption onto the resins were also obtained at optimized conditions.

The natural oil sands are always entrained with different chemicals, such as SiO₂, kaolinite, CaCl₂, and NaCl. During the extraction of oil sands, especially when the water is involved, these chemicals could be dissolved or dispersed into the solution. However, there is no information being published to give the effects of these materials on the adsorption of ionic liquids by the resins. Herein, the effects of these background chemicals in aqueous solution on adsorption of ILs have been investigated.

The adsorption amount of resin q (mg/g) and adsorption ratio A (%) of ILs were obtained according to Equations (2) and (3) [24,30]:

$$q = \frac{(C_0 - C)V}{m} \quad (2)$$

$$A = \frac{C_0 - C}{C_0} \times 100\% \quad (3)$$

where C_0 and C are the concentrations of ILs in the solution before and after the adsorption, respectively, mg/L; V stands for the volume of the solution, L; m represents the weight of the ion-exchange resin, g.

2.4. Regeneration and Reusing of Resins

The acid solution was used to regenerate the ion-exchange resin. When the ILs-loaded ion-exchange resin comes in contact with acid solution of high concentration, the adsorbed cation of IL will be replaced by the H⁺ in solution (Equation (4)). The cations will transport through the pores and

the boundary layer film of the resin. Consequently, the cations are transferred into the new solution. The ion-exchange resin is simultaneously regenerated and transformed to its original acidic form.



In regeneration experiments, the HCl solutions (30 mL) of 15 wt% were added into a flask with ILs-loaded ion-exchange resin. The mixture of resins and HCl solutions were stirred at 250 rpm under water bath of 60 °C for 30 min. Subsequently, the regenerated ion-exchange resins were separated from solutions through filtration and reused for the adsorption of fresh ILs solutions. The whole procedures for the removal of ILs from residual sands are shown in Figure 2.

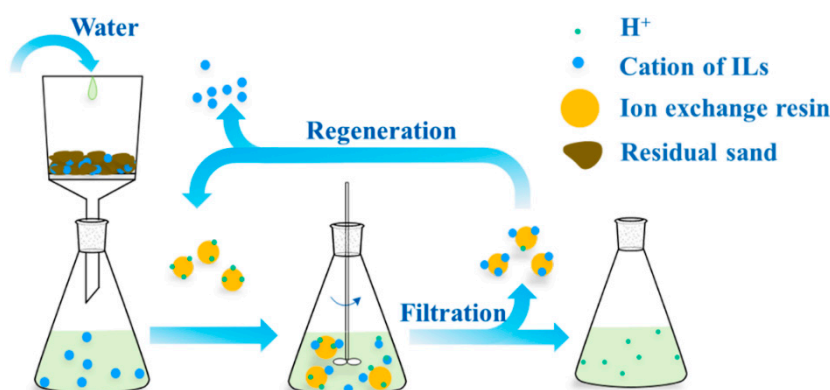


Figure 2. Schematic of the removal of ionic liquids from residual sands by washing–ion exchange combined process.

2.5. Instrumental Analysis

The elemental compositions of residual sands after water washing were analyzed by the PHILIPS XL30 environmental scanning electron microscopy (ESEM) with an energy disperse spectroscopy (EDS) detector.

The remaining ILs in residual sands and ion-exchange resins were characterized using a Bruker Tensor 27 Fourier transform infrared spectrometer (FTIR). Samples of residual sands were prepared by the pressed disk method. Spectroscopy of the ion-exchange resins was obtained by applying the diamond lens Attenuated Total Reflectance (ATR) module. Pure ionic liquid was characterized through liquid film method.

Concentrations of ILs in filtrate after adsorption were determined by using the Puxi TU-1901 UV-vis spectrophotometer. To obtain the calibration curve for quantitative computation, IL solutions with different concentrations (5–40 mg/L) were measured to obtain the calibration curve. The DI water was used as the reference solution. The 211 nm was determined to be the working wavelength based on the full-wave scanning. Finally, the calibration curve was used to calculate the ILs' concentration based on the absorbance of ILs solution [9].

3. Results and Discussion

3.1. Effect of Washing Times

The results of ESEM-EDS are shown in Table 3. A small amount of fluorine was detected in the residual sands after twice washing. This means that there still remained ILs in the residual sands. However, the fluorine was not detected in residual sands after washing for 3 or 4 times, suggesting no ILs anions were left in the residual solids. Figure 3 presents the results of infrared spectrum of the residual sands with different washing times after [Bmim][BF₄]-enhanced oil sands extraction. The residual sands without water washing displayed a peak at 1550–1600 cm⁻¹, which is the characteristic peak of the in-plane C–C of the imidazole ring. This proved the remaining of

ILs cations in the residual sands. However, it was found that this peak was absent for the residual sands which were washed for 3 and 4 times, indicating that there were no cations of ILs in the residual sands. The strong absorption band near 1100 cm^{-1} is the C–N stretching vibration of the cations of ILs, whereas it is also the characteristic peak of silicates in the residual sands. From the above results of ESEM-EDS and FTIR, it can be concluded that washing the residual sands for at least 3 times is required to remove ILs to aqueous solution completely. The ILs concentration in the filtrate after 3 times water washing was detected to be in the range of 8.02–10.69 g/L. Consequently, the concentration of the model ILs solution was determined to be 10 g/L.

Table 3. Elemental composition in the residual sands with different washing times after ionic liquids ([Bmim][BF₄] and [Emim][BF₄])-enhanced oil sands extraction.

ILs	Washing Times	Residual Sands (w/w %)				
		C	O	Si	Al	F
[Bmim][BF ₄]	2	5.6	51.6	38.5	3.0	1.3
	3	7.4	46.2	43.1	3.3	-
	4	10.5	43.1	39.4	7.0	-
[Emim][BF ₄]	2	6.5	47.3	38.9	6.0	1.3
	3	11.2	46.3	36.0	6.5	-
	4	12.1	42.5	43.5	1.9	-

–: undetected.

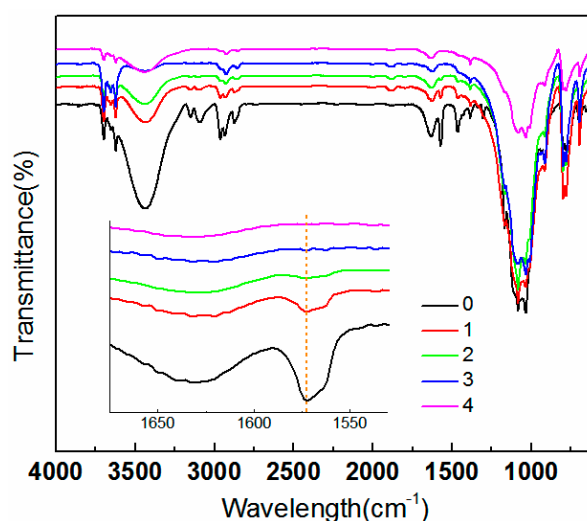


Figure 3. Infrared spectrum of the residual sands with different water washing times after ionic liquid ([Bmim][BF₄])-enhanced oil sands extraction.

3.2. Effect of Operation Parameters on ILs Adsorption

The resin dose is an important parameter to obtain the quantitative uptake of IL. Figure 4a shows the adsorption of [Bmim][BF₄] and [Emim][BF₄] as a function of the resin dose. It was indicated that the adsorption ratio of two ILs increased up to an optimum dosage (10 g), beyond which the removal efficiency (>90% for both ILs) did not significantly change. This is anticipated for a fixed initial IL concentration, because a higher amount of adsorbents provides more available exchangeable sites (or higher surface area) for the ions [31]. The maximum adsorption ratios were determined to be 95% and 90% for [Bmim][BF₄] and [Emim][BF₄], respectively, when the resin dosage was above 10 g. This resin dose was obtained as the optimal dosage for both ILs.

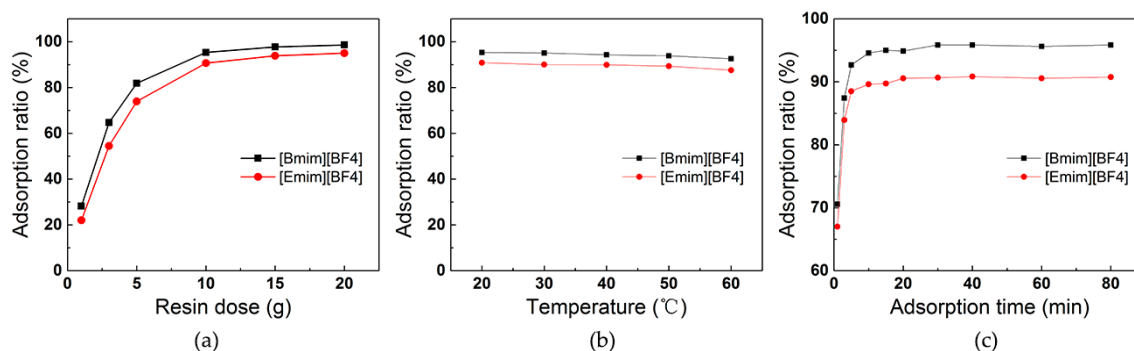


Figure 4. Effect of (a) resin dose; (b) temperature; (c) adsorption time on the adsorption ratio of ionic liquids ([Bmim][BF₄] and [Emim][BF₄]) onto ion-exchange resin (Amberlite IR 120Na).

The effect of temperature on the adsorption of ILs onto resins is shown in Figure 4b. For both [Bmim][BF₄] and [Emim][BF₄], the adsorption ratio decreased slightly (<4%) as adsorption temperature increased from 20 °C to 60 °C. It suggested that the [Bmim][BF₄] and [Emim][BF₄] ions were well accessible onto Amberlite IR 120Na adsorption sites at low temperature. A similar result has been obtained during the adsorption of benzothiazolium ionic liquid ([HBth][CF₃SO₃]) onto strongly acidic ion-exchange resin (732/H resin) [27]. This is different from those of some metal ions (e.g., Cu²⁺, Zn²⁺, Ni²⁺, Pb²⁺, and Cd²⁺) onto the resins (Dowex 50W [32], Amberlite IR 120Na [33]). The adsorption of these divalent metal ions was found to be an endothermic ion exchange process, which could be facilitated by increasing the temperature. However, herein, increasing the temperature played little role in the adsorption of ionic liquids by the resins, indicating the adsorption process of ionic liquids onto the resins would be an exothermic process [27].

The influence of contact time on the adsorption of two ILs is depicted in Figure 4c. At initial stages, the uptake of ILs was rapid. This is because all the resin sites are vacant at the beginning, hence the extent of adsorption is high [34]. Subsequently, due to the decrease in the number of adsorption sites as well as ILs concentration, the adsorption rate of ions on the resins became slow. After 30 min, no remarkable adsorption was observed for the two ILs, indicating the adsorption equilibrium was reached in 30 min. More than 95% of [Bmim][BF₄] and 90% of [Emim][BF₄] were adsorbed onto the resins when the equilibrium was attained.

3.3. Adsorption Isotherms

The adsorption isotherms can provide the adsorbate molecules distribution between the solid and liquid phases when the adsorption process reaches the equilibrium state. Herein, the Langmuir, Freundlich, and Sips models were used to analyze the equilibrium data obtained from ILs adsorption. The parameters, along with a correlation coefficient (R^2) of three isotherms, are given in Table 4. The fitting results are presented in Figure 5. The three adsorption models are given as Equations (5)–(7), respectively:

$$q_e = \frac{q_m K_L C_e}{1 + K_L C_e} \quad (5)$$

$$q_e = K_F C_e^{1/n} \quad (6)$$

$$q_e = \frac{q_m K_S C_e^{1/p}}{1 + K_S C_e^{1/p}} \quad (7)$$

where q_e is the equilibrium adsorption capacity, mg/g; C_e denotes the equilibrium concentration of ILs in solution, mg/L; q_m stands for the maximum adsorption capacity, mg/g; K_L is the Langmuir constant related to the affinity between the adsorbent and adsorbate, L/mg; K_F refers to the Freundlich constants correlated with the adsorption capacity for a unit equilibrium concentration, and $1/n$ is the

heterogeneity factor; K_S represents the Sips constant relating to the median binding affinity; $1/p$ stands for the heterogeneity factor varied from 0 to 1.

Table 4. Fitting parameters of isotherms (Langmuir, Freundlich, and Sips models) for adsorption of ionic liquids ([Bmim][BF₄] and [Emim][BF₄]) onto ion-exchange resin (Amberlite IR 120Na).

Ionic Liquids	Langmuir Model				Freundlich Model			Sips Model			
	q_m (mg/g)	K_L (mL/mg)	R_L	R^2	K_F	$1/n$	R^2	q_m (mg/g)	K_S (10^{-2})	$1/p$	R^2
[Bmim][BF ₄]	1577.7	4.24	0.105	0.96	144.3	0.300	0.98	2524.1	2.67	0.512	0.99
[Emim][BF ₄]	1365.8	2.31	0.178	0.98	81.5	0.341	0.98	2100.9	1.47	0.569	0.99

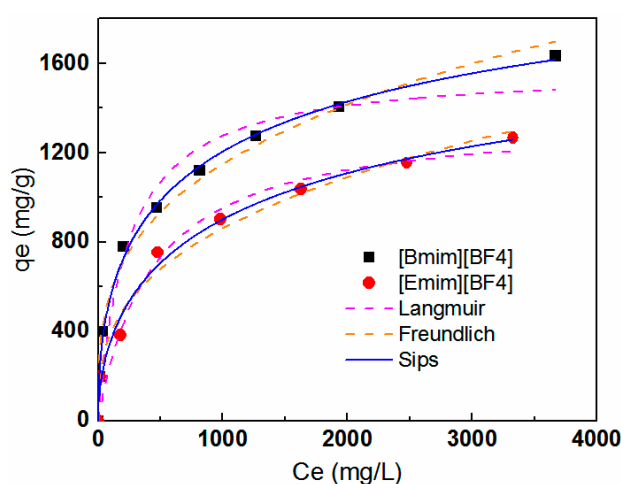


Figure 5. Langmuir, Freundlich, and Sips isotherms for adsorption of ionic liquids ([Bmim][BF₄] and [Emim][BF₄]) onto ion-exchange resin (Amberlite IR 120Na).

The Langmuir equation assumes homogeneous and monolayer adsorption, with no lateral interaction and steric hindrance between the adsorbed molecules [35]. The essential features and feasibility of the Langmuir model can be expressed by a dimensionless constant commonly known as separation factor [29], which is used to predict if an adsorption system is “favorable” or “unfavorable” (Equation (8)):

$$R_L = \frac{1}{1 + K_L C_0} \tag{8}$$

where R_L represents the separation factor; C_0 refers to the lowest initial concentration of ILs, mg/L. The value of R_L indicates the shape of isotherm to be either unfavorable ($R_L > 1$) or linear ($R_L = 1$) or favorable ($0 < R_L < 1$) or irreversible ($R_L = 0$). From Table 4, [Bmim][BF₄] showed a higher K_L value than that of [Emim][BF₄], which was in concert with the higher maximum adsorption capacity obtained from [Bmim][BF₄]. This suggested the higher affinity between the [Bmim][BF₄] and the resins compared with that of [Emim][BF₄]. Values of R_L were in range of 0 and 1 for two ILs, indicating that the ion-exchange resin is favorable for adsorption of two ILs under the conditions studied.

The Freundlich model can be applied to multilayer adsorption of adsorbate onto heterogeneous surface. It assumes that: (i) the heat of adsorption decreases with the increase of surface coverage of adsorbent; (ii) the binding sites on the surface have different adsorption energies [36]. As presented in Table 4, the K_F for [Bmim][BF₄] was higher than that for [Emim][BF₄]. This is in line with the results obtained from the Langmuir model, suggesting that the uptake is higher for IL with longer alkyl chain length of the imidazolium cation. Similar behavior was observed in the adsorption of ILs onto other adsorbents, such as activated carbons and soils [37,38]. The enhanced adsorption capacity for IL with longer alkyl chains is mainly attributed to higher van der Waals and polar interactions between the IL and the resins [25].

The value of $1/n$ is indicative of the type of adsorbate–adsorbent system as follows: irreversible ($1/n = 0$), favorable ($0 < 1/n < 1$), or unfavorable ($1/n > 1$). For [Bmim][BF₄] and [Emim][BF₄], the values of $1/n$ were 0.300 and 0.341, respectively, further proving that two ILs are adsorbed favorably by the ion-exchange resin during this study.

The Sips model is a composite of the Langmuir and Freundlich models with three parameters [39]. It can be employed to predict the heterogeneous adsorption systems and circumvent the limitation of the rising adsorbate concentration associated with the Freundlich isotherm [35]. For a homogeneous surface, $1/p$ is equal to 1, while when $1/n$ is between 0 and 1, this suggests the surface of adsorbent is heterogeneous [40]. It can be seen from Table 4 that the Sips model (with R² reaching 0.99) reproduced the adsorption experimental data better than the Langmuir and Freundlich models, which could also be demonstrated graphically in Figure 5. Accordingly, results suggested that the adsorption of [Bmim][BF₄] and [Emim][BF₄] onto the resins is probably controlled by a heterogeneous process [41].

3.4. Adsorption Kinetics

Besides adsorption equilibrium, the adsorption kinetics is another important aspect for parameter evaluation of the adsorption process, which is used to describe the solute uptake rate. Herein, the experimental data were analyzed by the pseudo-first- and the pseudo-second-order kinetic models. The nonlinear form is considered a better way to obtain the kinetic parameters [42], shown as Equations (9) and (10):

$$q_t = q_e(1 - e^{-k_1t}) \tag{9}$$

$$q_t = \frac{k_2q_e^2t}{1 + k_2q_e t} \tag{10}$$

where q_t denotes the amount of ILs adsorbed on the resins at any time, mg/g; q_e is the equilibrium adsorption capacity, mg/g; k_1 represents the pseudo-first-order rate constant, min⁻¹; t refers to the contact time, min; k_2 stands for the pseudo-second-order rate constant, g/(mg·min); $h = k_2q_e^2$ is defined as the initial adsorption rate constant.

The fitting parameters are summarized in Table 5, including uptakes of ILs at equilibrium state, adsorption rate constants, and correlation coefficients for the pseudo-first- and pseudo-second-order models. By comparing the values of R², it could be found that the pseudo-second-order model provided a better fit for two ILs' adsorption. The initial sorption rate, h , followed the order of [Bmim][BF₄] > [Emim][BF₄], which was in accordance with the affinity order observed in the equilibrium isotherm experiments [43]. In addition, Figure 6 shows the adsorbed amount of ILs as a function of contact time. The uptake of ILs increased quickly to over 70% of equilibrium adsorption capacity within 1 min. These findings suggested that the adsorption of ionic liquids on the resin is a fast process. It also indicated that the rate-determining step may be a chemical adsorption involving valence forces through exchanging of electrons between ILs cation and the resin [42].

Table 5. Fitting parameters of kinetics (pseudo-first- and pseudo-second-order models) for adsorption of ionic liquids ([Bmim][BF₄] and [Emim][BF₄]) onto ion-exchange resin (Amberlite IR 120Na).

Ionic Liquids	Pseudo-First-Order Model			Pseudo-Second-Order Model			
	$q_{e,cal}$ (mg/g)	k_1 (min ⁻¹)	R ²	$q_{e,cal}$ (mg/g)	k_2 (10 ⁻³ g/(mg·min))	h	R ²
[Bmim][BF ₄]	943.3	3.05	0.921	969.0	2.90	2722.9	0.984
[Emim][BF ₄]	895.8	3.07	0.945	919.3	3.14	2653.7	0.972

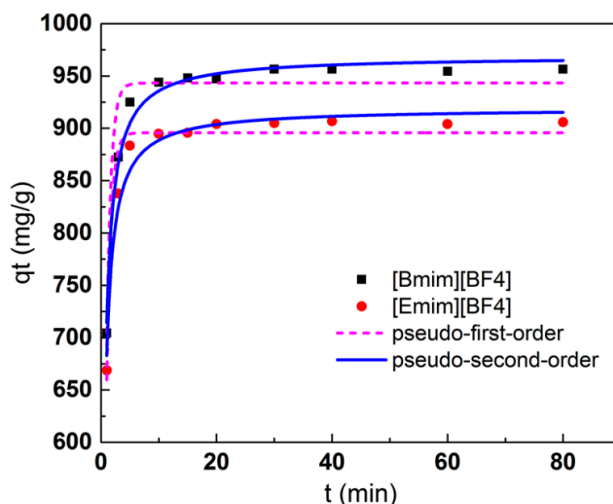


Figure 6. Pseudo-first- and pseudo-second-order kinetics for adsorption of ionic liquids ([Bmim][BF₄] and [Emim][BF₄]) onto ion-exchange resin (Amberlite IR 120Na).

3.5. Effect of Background Chemicals on ILs Adsorption

Actually, some chemicals or minerals of residual sands may enter the aqueous solution together with ILs in the washing process. Thus, it is necessary to investigate the effect of these chemicals or minerals on the adsorption process.

3.5.1. Effect of Silica and Kaolinite

The silica (SiO₂) and some clays, such as kaolinite (Al₄[Si₄O₁₀](OH)₈), illite (K_{1-1.5}Al₄[Si_{7-6.5}Al_{1-1.5}O₂₀](OH)₄), montmorillonite ((0.5Ca Na)_{0.7}(Al Mg Fe)₄[(Si Al)₈O₂₀]_n H₂O), and so forth, are common minerals in the unconventional oil ores [44,45]. As demonstrated in Figure 7a,b, the addition of SiO₂ and kaolinite exerted slight effect on the adsorption ratio of [Bmim][BF₄]. It implied that the entrance of a small amount of SiO₂ and kaolinite into the aqueous solution during the washing process would not influence the adsorption. The insignificant adsorption capacity of SiO₂ for ILs is mainly attributed to the relatively hydrophilic surfaces of minerals. The kaolinite is a layered aluminosilicate with 1:1 dioctahedral layered structure. Each layer consists of a sheet of SiO₄ tetrahedra connected via common oxygen atoms to a sheet of AlO₆ octahedra. The 1:1 layer cannot expand due to the hydrogen bonds between the two sheets [46]. As a result, the kaolinite exhibited a low adsorption potential for ILs.

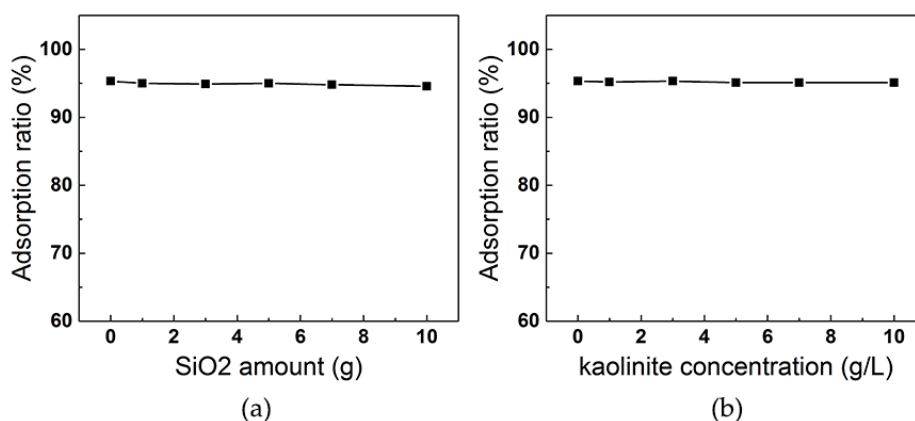


Figure 7. Effect of background chemicals (a) SiO₂, (b) kaolinite on the adsorption of ionic liquid ([Bmim][BF₄]) onto ion-exchange resin (Amberlite IR 120Na).

3.5.2. Effect of Ionic Strength

In practice, some natural ions are also involved during the washing step after the extraction of oil sands. Figure 8 shows the effects of CaCl_2 and NaCl on $[\text{Bmim}][\text{BF}_4]$ adsorption onto the resins. It was observed that the adsorption ratio of $[\text{Bmim}][\text{BF}_4]$ declined from 95.32% to 88.67% and 79.13%, respectively, when the concentrations of Ca^{2+} and Na^+ increased from 0 to 1000 ppm. The suppressed adsorption would be ascribed to the result of competitive adsorption of coexisting cations with $[\text{Bmim}]$ cations. Additionally, the divalent Ca^{2+} showed a more noticeable suppression of $[\text{Bmim}][\text{BF}_4]$ adsorption than that of monovalent Na^+ . This is mostly attributed to the stronger electrostatic attraction to ion-exchange resins. Thus, the Ca^{2+} ions would compete against the $[\text{Bmim}]$ cations for binding sites more effectively [47,48].

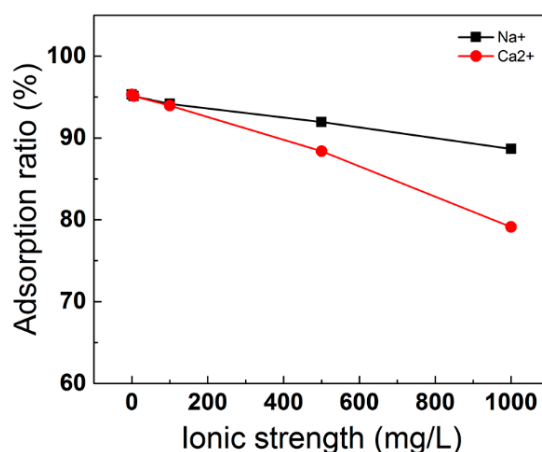


Figure 8. Effect of ionic strength on the adsorption of ionic liquid ($[\text{Bmim}][\text{BF}_4]$) onto ion-exchange resin (Amberlite IR 120Na).

3.6. Recyclability of Ion-Exchange Resins

The regeneration and reuse of saturated adsorbents are crucial for practical application. The effect of reusing times on adsorption performance of ion-exchange resin was investigated in repeated adsorption and desorption experiments. As illustrated in Figure 9, the adsorption capacity of ion-exchange resins slightly decreased after three times of reuse. Nevertheless, the adsorption ratio of $[\text{Bmim}][\text{BF}_4]$ could remain over 90% after reusing for three times. This implies that the Amberlite IR 120Na can be used as a stable and reusable adsorbent for the adsorption of ILs.

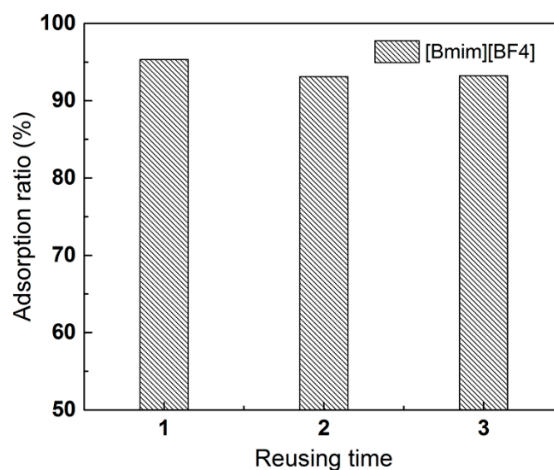


Figure 9. Effect of reusing times on the adsorption of ionic liquid ($[\text{Bmim}][\text{BF}_4]$) onto ion-exchange resin (Amberlite IR 120Na).

The loss of adsorption capacity is probably due to the fact that some binding sites might lose activity during the adsorption–desorption cycles, which could not allow further adsorption of the solutes [47]. Moreover, the adsorption sites of resins may be incompletely regenerated. These sites are still occupied with [Bmim] cations after regeneration and thus lose the adsorption ability in the next adsorption process. Remaining of ILs on the regenerated resin was evidenced by the FTIR results (Figure 10). The pure [Bmim][BF₄] is characterized by peaks at 1150~1200 cm⁻¹ (in-plane C–N of the imidazole ring), 1550~1600 cm⁻¹ (in-plane C–C of the imidazole ring), 2800~3000 cm⁻¹ (the C–H stretching vibrations of methyl and methylene groups), and 3100~3200 cm⁻¹ (the ring C–H stretching vibrations) [49]. The spectrum of ion-exchange resin showed a broad band located at 3414 cm⁻¹, which may be associated with the O–H stretching vibration of interlayer water molecules and the H-bonded OH groups [50]. The peak at 1572 cm⁻¹ was not observed for fresh resin while there was a weak transmittance in the spectrum of regenerated resin, indicating the presence of residual [Bmim] cations on the resin after regeneration.

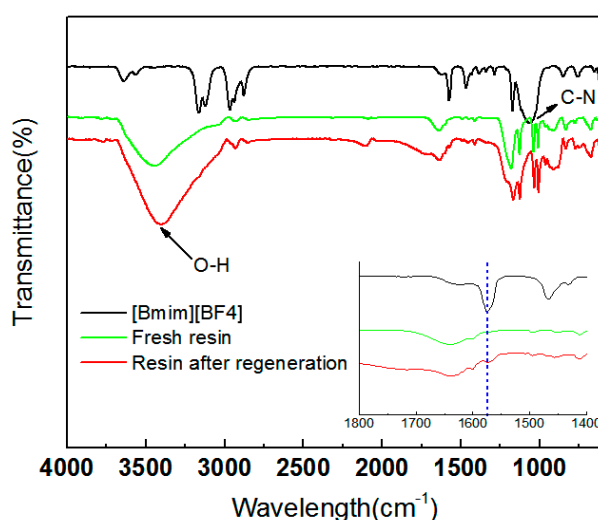


Figure 10. Infrared spectrum of pure [Bmim][BF₄] (black line), the fresh ion-exchange resin (Amberlite IR 120Na) (green line), and the ion-exchange resin after several times of regeneration (red line).

4. Conclusions

A washing–ion exchange combined method was proposed for the removal of ILs ([Bmim][BF₄] and [Emim][BF₄]) from the residual sands after the ILs-assisted solvent extraction of oil sands. At least 3 times of water washing was required to remove ILs from residual sands to the solution completely. Adsorption of two ILs onto ion-exchange resins was conducted in self-prepared ILs aqueous solution. It was found that over 90% of ionic liquids could be adsorbed by the resins at ambient conditions for 30 min. The adsorption of both ILs on Amberlite IR 120Na resin was found to be rate-controlled and could fit with the Sips isotherm. The increase of ionic strength in solution was evidenced to be deteriorative to the uptake of [Bmim][BF₄], whereas the existence of kaolinite and SiO₂ in the solution was proven to exert slight influence on the adsorption capacity of resins. The regeneration tests showed stable performance of ion-exchange resins after being reused for at least three times.

Author Contributions: H.S. designed the experiments; J.Z. carried out the experiments and wrote the manuscript; G.M. and Y.N. contributed to the analysis and interpretation of data; J.C. contributed the reagents/materials/analysis tools; L.H. revised the manuscript critically for important intellectual content; X.L. provided financial support and constructive comments on the revision.

Funding: This research was funded by National Natural Science Foundation of China grant number No. 41471258, No. 21506155. And the APC was funded by National Natural Science Foundation of China grant number No. 41471258.

Conflicts of Interest: There are no conflicts to declare.

References

1. Welton, T. Room-temperature ionic liquids. Solvents for synthesis and catalysis. *Chem. Rev.* **1999**, *99*, 2071–2083. [[CrossRef](#)] [[PubMed](#)]
2. Hallett, J.P.; Welton, T. Room-temperature ionic liquids: Solvents for synthesis and catalysis. 2. *Chem. Rev.* **2011**, *111*, 3508–3576. [[CrossRef](#)] [[PubMed](#)]
3. Huddleston, J.G.; Visser, A.E.; Reichert, W.M.; Willauer, H.D.; Broker, G.A.; Rogers, R.D. Characterization and comparison of hydrophilic and hydrophobic room temperature ionic liquids incorporating the imidazolium cation. *Green Chem.* **2001**, *3*, 156–164. [[CrossRef](#)]
4. Buszewski, B.; Studzińska, S. A review of ionic liquids in chromatographic and electromigration techniques. *Chromatographia* **2008**, *68*, 1–10. [[CrossRef](#)]
5. Sheldon, R. Catalytic reactions in ionic liquids. *Chem. Commun.* **2001**, *23*, 2399–2407. [[CrossRef](#)]
6. Li, X.; Sun, W.; Wu, G.; He, L.; Li, H.; Sui, H. Ionic liquid enhanced solvent extraction for bitumen recovery from oil sands. *Energy Fuel* **2011**, *25*, 5224–5231. [[CrossRef](#)]
7. Painter, P.; Williams, P.; Lupinsky, A. Recovery of bitumen from Utah tar sands using ionic liquids. *Energy Fuel* **2010**, *24*, 5081–5088. [[CrossRef](#)]
8. Painter, P.; Williams, P.; Mannebach, E. Recovery of bitumen from oil or tar sands using ionic liquids. *Energy Fuel* **2010**, *24*, 1094–1098. [[CrossRef](#)]
9. Li, X.; Wang, J.; He, L.; Sui, H.; Yin, W. Ionic liquid-assisted solvent extraction for unconventional oil recovery: Computational simulation and experimental tests. *Energy Fuel* **2016**, *30*, 7074–7081. [[CrossRef](#)]
10. Wang, W.; Ma, X.; Grimes, S.; Cai, H.; Zhang, M. Study on the absorbability, regeneration characteristics and thermal stability of ionic liquids for VOCs removal. *Chem. Eng. J.* **2017**, *328*, 353–359. [[CrossRef](#)]
11. Ahmad, W.; Ostonen, A.; Jakobsson, K.; Uusi-Kyyny, P.; Alopaeus, V.; Hyvääkö, U.; King, A.W.T. Feasibility of thermal separation in recycling of the distillable ionic liquid [DBNH][OAc] in cellulose fiber production. *Chem. Eng. Res. Des.* **2016**, *114*, 287–298. [[CrossRef](#)]
12. Blanchard, L.A.; Brennecke, J.F. Recovery of organic products from ionic liquids using supercritical carbon dioxide. *Ind. Eng. Chem. Res.* **2001**, *40*, 287–292. [[CrossRef](#)]
13. Mukesh, C.; Mondal, D.; Sharma, M.; Prasad, K. Rapid dissolution of DNA in a novel bio-based ionic liquid with long-term structural and chemical stability: Successful recycling of the ionic liquid for reuse in the process. *Chem. Commun.* **2013**, *49*, 6849–6851. [[CrossRef](#)] [[PubMed](#)]
14. Cláudio, A.F.M.; Marques, C.F.C.; Boal-Palheiros, I.; Freire, M.G.; Coutinho, J.A.P. Development of back-extraction and recyclability routes for ionic-liquid-based aqueous two-phase systems. *Green Chem.* **2014**, *16*, 259–268. [[CrossRef](#)]
15. Gutowski, K.E.; Broker, G.A.; Willauer, H.D.; Huddleston, J.G.; Swatloski, R.P.; Holbrey, J.D.; Rogers, R.D. Controlling the aqueous miscibility of ionic liquids: Aqueous biphasic systems of water-miscible ionic liquids and water-structuring salts for recycle, metathesis, and separations. *J. Am. Chem. Soc.* **2003**, *125*, 6632–6633. [[CrossRef](#)] [[PubMed](#)]
16. Wang, J.; Luo, J.; Zhang, X.; Wan, Y. Concentration of ionic liquids by nanofiltration for recycling: Filtration behavior and modeling. *Sep. Purif. Technol.* **2016**, *165*, 18–26. [[CrossRef](#)]
17. Wu, H.; Shen, F.; Wang, J.; Luo, J.; Liu, L.; Khan, R.; Wan, Y. Separation and concentration of ionic liquid aqueous solution by vacuum membrane distillation. *J. Membr. Sci.* **2016**, *518*, 216–228. [[CrossRef](#)]
18. Zhang, L.; Zhang, J.; Fu, H.; Zhang, H.; Liu, H.; Wan, Y.; Zheng, S.; Xu, Z. Microporous zeolite-templated carbon as an adsorbent for the removal of long alkyl-chained imidazolium-based ionic liquid from aqueous media. *Microporous Mesoporous Mater.* **2018**, *260*, 59–69. [[CrossRef](#)]
19. Lemus, J.; Moya, C.; Gilarranz, M.A.; Rodriguez, J.J.; Palomar, J. Fixed-bed adsorption of ionic liquids onto activated carbon from aqueous phase. *J. Environ. Chem. Eng.* **2017**, *5*, 5347–5351. [[CrossRef](#)]
20. Lemus, J.; Palomar, J.; Gilarranz, M.A.; Rodriguez, J.J. On the kinetics of ionic liquid adsorption onto activated carbons from aqueous solution. *Ind. Eng. Chem. Res.* **2013**, *52*, 2969–2976. [[CrossRef](#)]
21. Palomar, J.; Lemus, J.; Gilarranz, M.A.; Rodriguez, J.J. Adsorption of ionic liquids from aqueous effluents by activated carbon. *Carbon* **2009**, *47*, 1846–1856. [[CrossRef](#)]
22. Min, Y.; Zhou, Y.; Zhang, M.; Qiao, H.; Huang, Q.; Ma, T. Removal of ionic liquid by engineered bentonite from aqueous solution. *J. Taiwan Inst. Chem. E* **2015**, *53*, 153–159. [[CrossRef](#)]

23. Won, S.W.; Choi, S.B.; Mao, J.; Yun, Y.S. Removal of 1-ethyl-3-methylimidazolium cations with bacterial biosorbents from aqueous media. *J. Hazard. Mater.* **2013**, *244–245*, 130–134. [[CrossRef](#)] [[PubMed](#)]
24. Choi, S.B.; Won, S.W.; Yun, Y.-S. Use of ion-exchange resins for the adsorption of the cationic part of ionic liquid, 1-ethyl-3-methylimidazolium. *Chem. Eng. J.* **2013**, *214*, 78–82. [[CrossRef](#)]
25. Li, L.; Wang, Y.; Qi, X. Adsorption of imidazolium-based ionic liquids with different chemical structures onto various resins from aqueous solutions. *RSC Adv.* **2015**, *5*, 41352–41358. [[CrossRef](#)]
26. Ma, C.H.; Zu, Y.G.; Yang, L.; Li, J. Two solid-phase recycling method for basic ionic liquid [C₄mim]AC by macroporous resin and ion exchange resin from schisandra chinensis fruits extract. *J. Chromatogr. B* **2015**, *976–977*, 1–5. [[CrossRef](#)] [[PubMed](#)]
27. He, A.; Dong, B.; Feng, X.; Yao, S. Recovery of benzothiazolium ionic liquids from the coexisting glucose by ion-exchange resins. *J. Mol. Liq.* **2017**, *227*, 178–183. [[CrossRef](#)]
28. Liu, W.; Zhao, T.; Zhang, Y.; Wang, H.; Yu, M. The physical properties of aqueous solutions of the ionic liquid [Bmim][BF₄]. *J. Solut. Chem.* **2006**, *35*, 1337–1346. [[CrossRef](#)]
29. Vasiliu, S.; Bunia, I.; Racovita, S.; Neagu, V. Adsorption of cefotaxime sodium salt on polymer coated ion exchange resin microparticles: Kinetics, equilibrium and thermodynamic studies. *Carbohydr. Polym.* **2011**, *85*, 376–387. [[CrossRef](#)]
30. Shek, T.; Ma, A.; Lee, V.; McKay, G. Kinetics of zinc ions removal from effluents using ion exchange resin. *Chem. Eng. J.* **2009**, *146*, 63–70. [[CrossRef](#)]
31. Bayramoglu, G.; Altintas, B.; Arica, M.Y. Adsorption kinetics and thermodynamic parameters of cationic dyes from aqueous solutions by using a new strong cation-exchange resin. *Chem. Eng. J.* **2009**, *152*, 339–346. [[CrossRef](#)]
32. Pehlivan, E.; Altun, T. The study of various parameters affecting the ion exchange of Cu²⁺, Zn²⁺, Ni²⁺, Cd²⁺, and Pb²⁺ from aqueous solution on dowex 50w synthetic resin. *J. Hazard. Mater.* **2006**, *134*, 149–156. [[CrossRef](#)] [[PubMed](#)]
33. Demirbas, A.; Pehlivan, E.; Gode, F.; Altun, T.; Arslan, G. Adsorption of Cu(ii), Zn(ii), Ni(ii), Pb(ii), and Cd(ii) from aqueous solution on Amberlite IR-120 synthetic resin. *J. Colloid Interface Sci.* **2005**, *282*, 20–25. [[CrossRef](#)] [[PubMed](#)]
34. Naushad, M.; Alothman, Z.A.; Sharma, G. Kinetics, isotherm and thermodynamic investigations for the adsorption of Co(ii) ion onto crystal violet modified Amberlite IR-120 resin. *Ionics* **2014**, *21*, 1453–1459. [[CrossRef](#)]
35. Foo, K.Y.; Hameed, B.H. Insights into the modeling of adsorption isotherm systems. *Chem. Eng. J.* **2010**, *156*, 2–10. [[CrossRef](#)]
36. Freundlich, H.M.F. Uber die adsorption in losungen. *Z. Phys. Chem.* **1906**, *57*, 385–470. [[CrossRef](#)]
37. Ushiki, I.; Tashiro, M.; Smith, R.L. Measurement and modeling of adsorption equilibria of imidazolium-based ionic liquids on activated carbon from aqueous solutions. *Fluid Phase Equilib.* **2017**, *441*, 17–23. [[CrossRef](#)]
38. Stepnowski, P.; Mrozik, W.; Nichthauser, J. Adsorption of alkylimidazolium and alkyipyridinium ionic liquids onto natural soils. *Environ. Sci. Technol.* **2007**, *41*, 511–516. [[CrossRef](#)] [[PubMed](#)]
39. Sips, R. Combined form of langmuir and freundlich equations. *J. Chem. Phys.* **1948**, *16*, 490–495. [[CrossRef](#)]
40. Umpleby, R.J.; Baxter, S.C.; Chen, Y.; Shah, R.N.; Shimizu, K.D. Characterization of molecularly imprinted polymers with the langmuir–freundlich isotherm. *Anal. Chem.* **2001**, *73*, 4584–4591. [[CrossRef](#)] [[PubMed](#)]
41. Yu, F.; Sun, L.; Zhou, Y.; Gao, B.; Gao, W.; Bao, C.; Feng, C.; Li, Y. Biosorbents based on agricultural wastes for ionic liquid removal: An approach to agricultural wastes management. *Chemosphere* **2016**, *165*, 94–99. [[CrossRef](#)] [[PubMed](#)]
42. Ho, Y.-S. Second-order kinetic model for the sorption of cadmium onto tree fern: A comparison of linear and non-linear methods. *Water Res.* **2006**, *40*, 119–125. [[CrossRef](#)] [[PubMed](#)]
43. Li, L.; Liu, F.; Jing, X.; Ling, P.; Li, A. Displacement mechanism of binary competitive adsorption for aqueous divalent metal ions onto a novel ida-chelating resin: Isotherm and kinetic modeling. *Water Res.* **2011**, *45*, 1177–1188. [[CrossRef](#)] [[PubMed](#)]
44. Hepler, L.G.; Smith, R.G. *The Alberta Oil Sands: Industrial Procedures for Extraction and Some Recent Fundamental Research*; AOSTRA Technical Publication Series #14; Alberta Oil Sands Technology and Research Authority: Edmonton, AB, Canada, 1994.
45. Dang-Vu, T.; Jha, R.; Wu, S.-Y.; Tannant, D.D.; Masliyeh, J.; Xu, Z. Wettability determination of solids isolated from oil sands. *Colloid Surf. A* **2009**, *337*, 80–90. [[CrossRef](#)]

46. Matzke, M.; Thiele, K.; Muller, A.; Filser, J. Sorption and desorption of imidazolium based ionic liquids in different soil types. *Chemosphere* **2009**, *74*, 568–574. [[CrossRef](#)] [[PubMed](#)]
47. Zhang, L.; Cao, W.; Alvarez, P.J.J.; Qu, X.; Fu, H.; Zheng, S.; Xu, Z.; Zhu, D. Oxidized template-synthesized mesoporous carbon with ph-dependent adsorption activity: A promising adsorbent for removal of hydrophilic ionic liquid. *Appl. Surf. Sci.* **2018**, *440*, 821–829. [[CrossRef](#)]
48. Lan, Q.; Bassi, A.S.; Zhu, J.-X.; Margaritis, A. A modified langmuir model for the prediction of the effects of ionic strength on the equilibrium characteristics of protein adsorption onto ion exchange/affinity adsorbents. *Chem. Eng. J.* **2001**, *81*, 179–186. [[CrossRef](#)]
49. Wu, J.; Wang, M.-J.; Stark, J.P.W. Evaluation of band structure and concentration of ionic liquid bmimbf4 in molecular mixtures by using second derivatives of ftir spectra. *J. Quant. Spectrosc. Radiat. Transf.* **2006**, *102*, 228–235. [[CrossRef](#)]
50. Elabd, A.A.; Zidan, W.I.; Abo-Aly, M.M.; Bakier, E.; Attia, M.S. Uranyl ions adsorption by novel metal hydroxides loaded Amberlite IR 120. *J. Environ. Radioact.* **2014**, *134*, 99–108. [[CrossRef](#)] [[PubMed](#)]



© 2018 by the authors. Licensee MDPI, Basel, Switzerland. This article is an open access article distributed under the terms and conditions of the Creative Commons Attribution (CC BY) license (<http://creativecommons.org/licenses/by/4.0/>).